1988

Deep Foundations on Bored and Auger Piles, Van Impe (ed.)
© 1988 Balkema, Rotterdam, ISBN 90 6191 814 6

Prediction of the load-settlement characteristics of bored piles

I.Luker
University of the Witwatersrand, RSA

ABSTRACT: A Method of modelling the soil-structure interaction is described, in which the soil displacement is divided between a boundary layer and an outer soil region. Shear box test results are recommended for the boundary layer behaviour, and a hyperbolic shear stress-strain function for the outer region. A simple computer-based method calculates and combines the displacements. Comparisons between field tests and theoretical predictions are made.

1 INTRODUCTION

There have been two fundamental approaches to predicting the load-settlement characteristics of piles. The first considers the distortion of the whole body of soil caused by the movement of the cylinder within it, and the second considers only the stresses and movements at the soil-pile interface, the rest of the soil being considered to be a rigid body.

Typical of the first approach are: (i) integration of Mindlin's equation for a pile divided into elements (e.g. Poulos and Davis 1968); (ii) closed form equations for the complete pile, (e.g. Randolph and Wroth 1978); (iii) the finite element method. Typical of the second approach is, for a pile divided into elements, to determine the loads and movements at each element that are compatible both with equilibrium and with an assumed shear stress - movement relationship at the soil-pile interface. (E.g. Seed and Reese 1957).

Researchers starting with the first approach have also included special provision for an assumed shear stress - movement relationship at the interface. For example a rigid, perfectly plastic shape of graph (Poulos and Davis (1968), and a graph that rises linearly to a peak, then falls instantaneously to a residual shear value, (Murff 1980).

The method described in this paper enables any form of shear stress - movement relationship at the interface to be used, and combines it with the simplest of the methods for calculating the movement of the rest of the soil body, that of Randolph and Wroth (1978).

2. MODEL OF SOIL/PILE BEHAVIOUR EMPLOYED

2.1 General description

The soil behaviour is characterised into 3 zones as shown in Fig. 1:

(i) A boundary layer adjacent to the pile shaft;

(ii) the rest of the soil extending radially away from the shaft;

(iii) the soil below a plane through the toe of the pile. The pile length is divided into discrete elements as shown in figure 1, which enables the soil properties in zones (i)and (ii) to vary with depth.

The method of analysis is of an iterative type, but is sufficiently

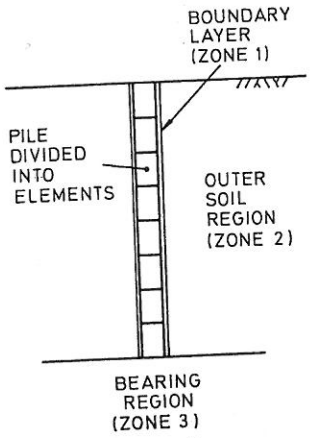

Fig. 1 - Characteristics of the soil/pile representation

simple to enable an IBM PC to compute the load-settlement relationship for a pile within two minutes. Its basic sequence of operations is as follows:

1. Apply pile head load to the first element.
2. Calculate the compression of the first element, temporarily disregarding the soil, and assuming that the bottom end of the element is rigidly supported.
3. Calculate the shear stress developed on the pile surface corresponding to the movement of the mid-length of the element calculated in step 2. (More information on how the shear stress is calculated is given in section 2.2).
4. Calculate the force corresponding to the surface shear stress on the element, then deduct it from the applied force at the top of the element to get the force at the bottom.
5. If force does exist at the bottom of the element, (i.e. the load shed via shear stress is less than the applied force), then apply this bottom force to the second element. Calculate the second element's mid point compression movement as described in step 2.
6. Sum the total compressions of the second and first elements to get the movement of the first element.
7. Calculate the surface shear stresses corresponding to the element movements in the same way as step 3.
8. Starting at the head of the pile, deduct from the applied load the forces shed via surface stress on each element.
9. While excess force continues to exist at the bottom of the elements currently included, continue to add on further elements until the toe of the pile is reached.
10. Calculate the movement of the toe of the pile, under the excess force acting there, using an elastic-perfectly plastic model for the soil in zone 3. (Further information is given in section 2.4).
11. The pile toe movement is then added to the compression movements of all the elements above it, in the same way as step 6.
12. Iterate through calculations of movement, surface shear stress and element forces until stability of these three parameter values is obtained for all elements and the toe.

For a given applied load to the pile, there are three possible conclusions to the calculations sequence 1-12 described above:

(i) The applied load is carried by the shaft surface shear stress only, and no force reaches the toe.

(ii) The applied load is carried by a combination of shaft and endbearing resistance.

(iii) The ultimate resistance of the shaft and endbearing are less than the applied load. (This would be shown by the failure of the iterations described in step 12 to converge).

A convenient algorithm that can easily be programmed to determine the ultimate capacity of a pile is to increase the applied load in intervals until a value fits category (iii) above. The last interval of increase of applied load is then progressively subdivided until a value sufficiently close to the pile's ultimate capacity is found.

2.2 Calculation of surface shear stress

The total movement of any element of the pile is calculated as described in steps 2,6 and 11 of section 2.1. This movement is split between that which occurs in the boundary layer (zone 1) and that in the outer region (zone 2).

The relationship between shear stress and movement in the boundary layer is anything chosen by the pile designer. For example the graphs in figure 2. Hence providing the proportion of the total movement that occurs in the boundary layer is known, the shear stress developed for that movement can be easily calculated.

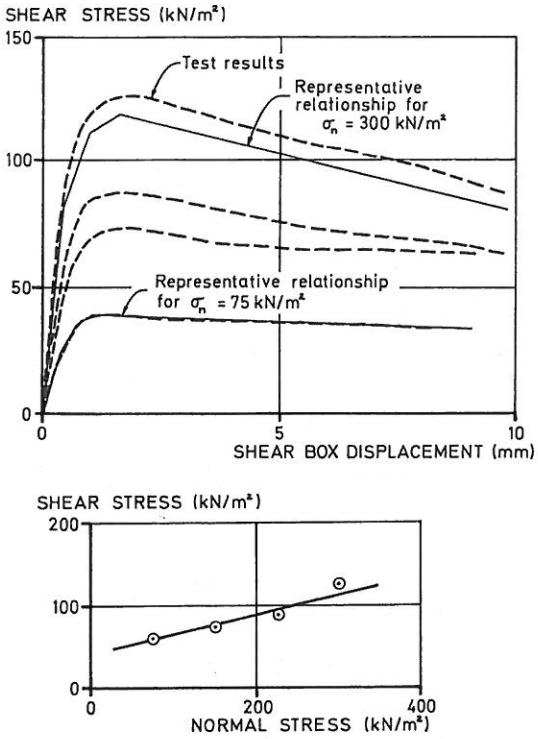

Fig. 2 - Representation of pile boundary layer behaviour from shear box test results

The proportional split between boundary layer and outer region is established before the numerical analysis sequence described in steps 1 to 12 is begun. For each element, the chosen τ_B-Δ_B relationship is divided into intervals, as shown in figure 3, giving corresponding values of τ_B and Δ_B. The displacement of the outer soil region, Δ_{rB}, for the applied value of τ_B is then calculated in the

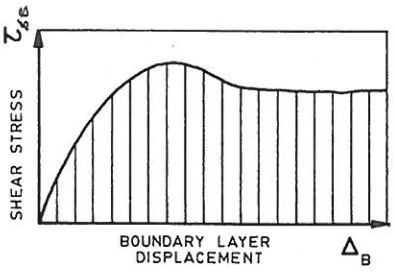

Fig. 3 - Typical shear stress-movement relationship for an element in the boundary layer

manner described in section 2.3. Corresponding values of total movement, Δ_s (= Δ_B + Δ_{rB}), and boundary layer movement, Δ_B, are therefore established. For any value of total movement, the boundary layer movement is found using interpolation between the established values.

2.3 Calculation of soil movement in the outer region.

This calculation may be done in any way chosen by the pile designner. However, a method is recommended here that has the advantages of simplicity and accurate reproduction of measured movements. The outer soil region movement is modelled as the elastic deformation of concentric cylinders as shown in figure 4, (Randolph and Wroth 1978) but with a hyperbolic relationship between shear stress and strain to give individual values of the elastic shear modulus, G, for each annular ring.

Referring to figure 5, for a short interval of radius δr:

$$\Delta_r/\delta r = \gamma = \tau_r/G \quad .....(1)$$

Where:
γ = shear strain
τ_r = shear stress at radius r
G = shear modulus applicable to the soil region.

From equilibrium, $\tau_r = \tau_o r_o/r$

$$\therefore \quad \Delta_r = \frac{\delta r \tau_o r_o}{Gr} \quad .....(2)$$

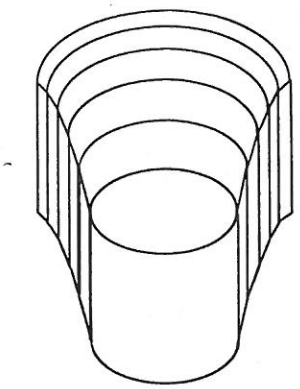

Fig 4. - Representation of soil movement in the outer region

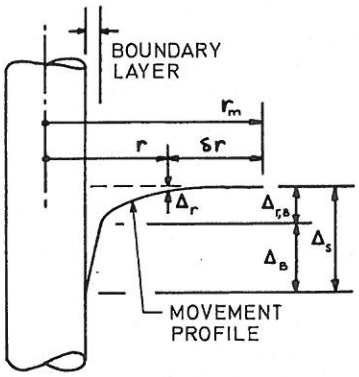

Fig. 5 - Representation of soil displacement

The hyperbolic shear stress-strain relationship is illustrated on the τ-γ axes of figure 6 and given by:

$$\tau = \gamma/(1/G_{init} + \gamma/\tau_{asymp}).$$

The secant shear modulus is then given by:

$$G = \frac{\delta\tau}{\delta\gamma} = 1/(1/G_{init} + \delta\gamma/\tau_{asymp}) \quad .....(3)$$

For a short interval of radius of δr : $\delta\gamma = \Delta_r/\delta r$

Substituting the expression for G from equation (3) into equation (2) gives:

$$\Delta_r = \frac{\delta_r/G_{init}}{(r/\tau_o r_o - 1/\tau_{asymp})} \quad .....(4)$$

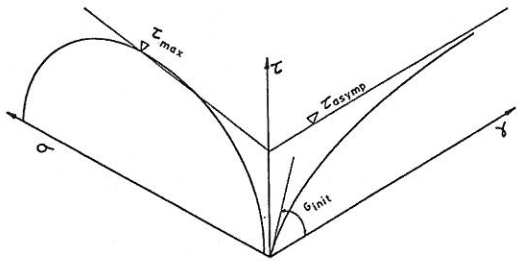

Fig. 6 - Hyperbolic shear stress-strain relationship

The total displacement of the outer soil region, $\Delta_{r,B}$ on figure 5, is then obtained by summing Δ_r for a series of intervals δ_r from the radius r_m, (where negligible displacement occurs), to the edge of the boundary layer on the pile.

The magnitude of r_m is significant in its effect on $\Delta_{r,B}$ when a fixed value of G is used for the whole outer soil region, and Randolph and Wroth suggest that r_m can be chosen empirically as $r_m = 2{,}5\ell(1-\nu)$. However, it is very much less significant when the realistic variation of G with shear strain that is given by the hyperbolic shear function is used.

The method of determining r_m that is recommended in this paper is to start with a low value and progressively increase it, calculating $\Delta_{r,B}$ for each r_m value until the change in $\Delta_{r,B}$ becomes negligibly small for an increment of r_m. This seems at first sight to be a tedious task but it is easily included in the computer program which does the rest of the calculations described in this paper, and adds only a few seconds to the total time for the analysis.

2.4 Endbearing load-displacement relationship

Here the recommendation of Randolph and Wroth is followed. That is to

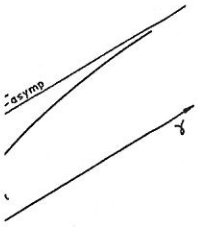

ear stress-

of the outer
igure 5, is
ng Δ_r for a
from the
gible
o the edge
on the pile.
is signifi-
$\Delta_{r,B}$ when a
ed for the
, and
gest that r_m
lly as r_m =
is very much
he realistic
ear strain
yperbolic
ining r_m that
paper is to
and progres-
lculating $\Delta_{r,B}$
l the change
ibly small
. This seems
tedious task
ded in the
does the
as described
s only a few
ime for the

splacement

n of Randolph
That is to

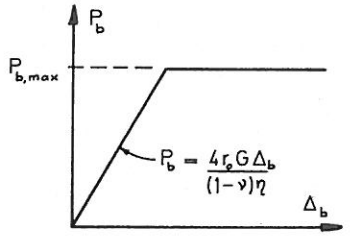

Fig. 7 - Endbearing load-settlement relationship

use the expression for the impression of a rigid punch onto the surface of an elastic medium:

$$\Delta_b = \frac{P_b(1-\upsilon)\,\eta}{4r_o G} \quad \ldots\ldots\ldots\ldots\ldots (5)$$

Where:

Δ_b = displacement of pile base
P_b = load on pile base
ν = Poisson's ratio
r_o = pile radius
G = representative secant shear modulus
η = factor to take account of rigidity of overburden above base level
= 1 for increments of pile load where part of the increment is carried by the shaft
= 0,85 when all the increment goes on the base

A limit to the load that can be carried by the pile base is imposed, as shown in figure 7.

$P_{b,\,ult}$ is given by the well known expression:

$$P_{b,\,ult} = cN_c + \gamma \ell N_q \quad \ldots(6)$$

3. DETERMINATION OF PILE AND SOIL PARAMETERS

3.1 Pile compressibility

For long piles, the pile compressibility has a significant effect on the load-deflection stiffness of the whole soil-pile system. Because of the creep of concrete under compressive load, care must be exercised in the choice of the elastic modulus to be used in the analysis. For example, if the predictions of the analysis are to be compared to a short term load test, a different concrete modulus would be used from that needed to predict long term settlements.

For piles made of ordinary concrete, it will not normally be necessary to do modulus tests on the concrete. There are sufficient empirical correlations between crushing strength and elastic modulus to enable the modulus to be estimated with sufficient accuracy.

3.2 Boundary layer shear stress - displacement parameters

During construction of the pile, the soil in the boundary layer is first of all removed by the auger and stands under zero stress. It is then subjected to the hydrostatic pressure of the concrete.

After the concrete has hardened, creep of the soil will probably reimpose on the pile the original stresses that existed in the ground before the hole was drilled.

The method used by the present author to determine the boundary layer characteristics is first to carry out four direct shear tests on remoulded samples of the soil, under a range of normal stresses. When all four shear stress-displacement graphs are plotted together, and a Coulomb envelope has been drawn through the shear stress - normal stress graph points, it is possible to produce two representative shear stress - displacement graphs for values of normal stress that are close to the range of radial stress that the pile will be subjected to. Figure 2 illustrates this process.

The radial stress on the pile is the most difficult parameter to estimate. As the following example shows, success has been obtained by using a value of K_o found from a self-boring pressuremeter test. The computer program calculates the radial stress on each element of the pile from the overburden stress multiplied by K_o. The boundary layer shear stress - displacement relationship for each element's value of radial stress is then automatically interpolated between the two representative graphs from the shear box tests.

3.3 Outer soil region shear stress-strain parameters

Figure 6 shows that three parameters are needed to define this relationship:

(i) The initial shear modulus G_{init}

(ii) The asymptotic value of shear stress, τ_{asymp}.

(iii) The rate of increase of τ_{asymp} with confining stresses.

The parameter τ of figure 6 is the shear stress acting on the cylindrical surfaces of the annular rings of soil shown in figure 4. For the hyperbolic function to represent the proportions of the shear stress-strain relationship for soil, τ_{asymp} must be higher than τ_{peak} for the soil. It is convenient, when interpreting in-situ tests to obtain the τ-γ graph parameters, to take $\tau_{asymp} = \tau_{max} = (\sigma_1 - \sigma_3)/2$. This choice leads to higher ratios of τ_{max}/τ_{peak} for high ϕ soils, giving a "stiffer" shape to the hyperbolic function, which is a true reflection of their physical behaviour. For these two reasons, τ_{asymp} is taken as equal to $(\sigma_1 - \sigma_3)/2$. The rate of increase of τ_{asymp} with confining stress is adequately modelled by the Mohr-Coulomb yield criterion, from the geometry of which we have:

$$\tau_{asymp} = c.\cos\phi + \frac{(\sigma_1 + \sigma_3)\sin\phi}{2} \quad (7)$$

Where σ_1 and σ_3 are the geostatic vertical and horizontal stresses in the ground.

The in-situ stiffness parameter G_{init} needs to be determined at very low strains on the undisturbed soil. Jardine et al (1985) have shown that this can be done in the laboratory, if accurate strain measurements are made on the specimen. Values obtained in this way by Jardine et al were high enough to agree well with values from geophysical methods and careful back-analysis of plate bearing and pile tests.

The value of G_{init} used in the example described in section 4 has been found from a new method of interpretation of the pressuremeter proposed by the present author. Details of this will be published separately but a brief description is that it consists of modelling the soil with discrete annular rings, in each of which the shear behaviour is represented by the hyperbolic function described in this paper, and the behaviour under the isotropic portion of the stress is represented by the result of a laboratory isotropic consolidation test. The method is characterised by a progressive relaxation method of numerical analysis that enables the size of the zone of soil affect-ed by the pressuremeter test to be determined.

3.4 Soil Under Pile Base

The range of strain over which the soil under the pile base is subjected is such that empirical values for a representative secant value of G are available in the literature. (e.g. Cernica 1982 and Lee et al 1983). Alternatively, in situ tests such as the pressuremeter or screw plate can be interpreted with the elastic model, over the relevant range of strain, to give a more accurate value of G_{sec}.

When the loading period is such that the volume change characteristics of the soil are needed, these can be included either as ν (as is the case in equation 5), or as the secant bulk modulus K, over the relevant range of strain. As for G, these can be obtained either from empirical correlations with other soil properties, or from tests. It is postulated by the present author that the isotropic consolidation test may give values of K that are less sensitive to sample disturbance than the shear parameters, and therefore that laboratory tests are adequate to find K. However this suggestion requires further investigation.

The shear strength parameters c and ϕ needed to predict the limiting endbearing stress using equation 6, can be found by normal means.

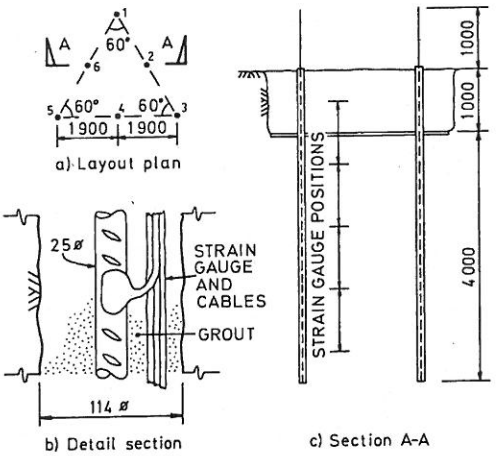

Fig. 8 - Details of test piles

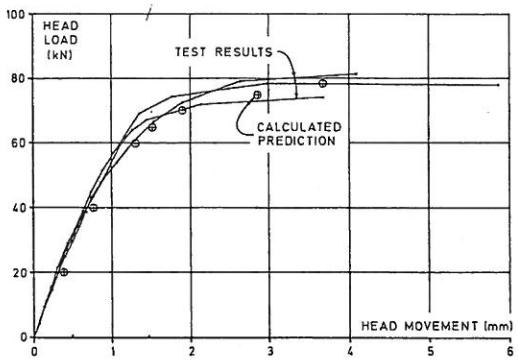

Fig. 9 - Head load v. deflection for all three piles

4. COMPARISON TO TEST RESULTS

Six small slender piles were constructed in an overconsolidated clay, in the triangular pattern shown in figure 8(a). The section of the pile is shown in Figure 8(b) and (c). Pile numbers 1, 3 and 5 were then used to provide reaction to a beam, to enable numbers 2, 4 and 6 to be loaded. All the piles were constructed identically and the soil deposit, (the Gault clay at Cambridge, England), was very uniform over the area of the tests.

Strain gauges were attached to the reinforcing steel at five points. After excavation of the top 1m of soil, which was highly weathered, the upper strain gauge position was exposed, and enabled a check to be made on the pile stiffnesses predicted from compression tests on specimens of the cement grout. Using these stiffnesses, the strain readings were converted into forces in the pile, and from those, the average shear stresses between strain measurement points were calculated.

Figure 9 shows that the variation between the load-settlement characteristics of the three piles was small. The variation of load down the piles was similarly close, but slightly greater variation was seen in the development of shear stress with increasing load. However, by calculating the average of the shear stress from the three piles, it is believed that a good representation is obtained for comparison to predicted values. The measured distribution of shear stress along the pile, as shown in figure 10(a), seems to be the best method of demonstrating the soil-pile interaction behaviour.

From Figure 10(a), it can be seen that at low percentages of ultimate load, the shear stress distribution is quite uniform, but with slightly higher stress near the top. This is caused by the fact that a large proportion of the applied load can be carried by the upper part of the pile, and hence forces and elastic compressions of the lower part are relatively small. At high percentages of the applied load, two changes in the stress distribution occur: (i) greater movement in the lower pile region, together with the stiffer shear stress-movement and higher ultimate shear stress values found under the higher pressure at greater depths, (refer figure 5), combine to cause the shear stresses on the lower pile to be greater than the upper; (ii) the movement of the upper pile region is sufficient to bring it into the strain softening region, and hence the shear stress has decreased slightly from previous values.

The methods of determination of the parameters needed for the model of the soil-pile system have been outlined in section 3. Boundary layer parameters are shown on figure 2, which is the result of consolidated quick direct shear tests on a remoulded sample of the

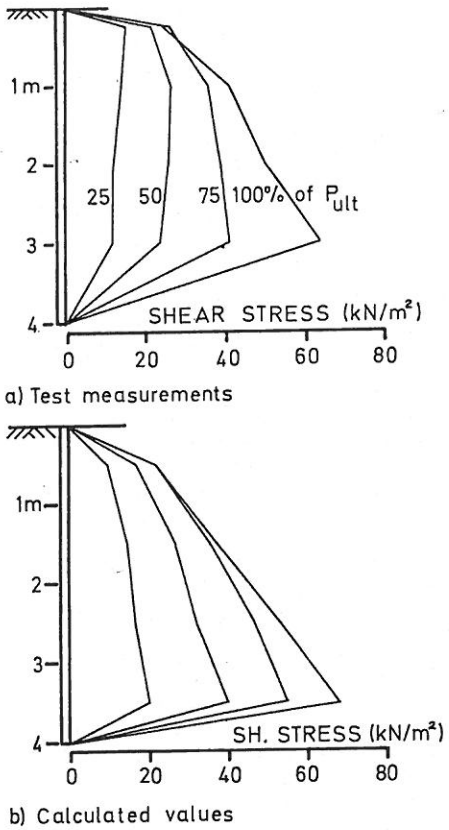

Fig. 10 - Shear stress distributions on the pile

clay from the site.

Shear distortion of the outer soil region, (Zone 2), would be undrained because of the short time (20 minutes) taken for the test. Kay and Parry (1982) give profiles of undrained shear strength against depth from two types of triaxials and three types of in-situ test on the same site. To represent the mean of these profiles of strength gain with depth, the parameters $c = 56kN/m^2$ and $\phi = 44°$ are appropriate.

The parameter G_{init} obtained from the new method of pressuremeter interpretation mentioned in section 3, was $60MN/m^2$. This is equivalent to a value of $E/c_u = 1600$, which is appropriate for "initial", (i.e. very low strain), soil deformation conditions. (Jardine et al 1985).

For the soil deformation under the pile base, an E/c_u value of 200 is appropriate because of the much greater range of strain experienced up to failure. From the data of Kay and Parry, and recognising that $G = E/3$ for an undrained soil, we have $G = 9MN/m^2$.

Ultimate endbearing strength from the Kay and Parry data with equation 6 is $1,3MN/m^2$.

The predicted load-settlement relationship is shown on figure 9, and is adequately close to the actual values for the majority of design purposes. Figure 10 compares the actual to predicted shear stress distributions. They are basically similar, but differ mainly at the top of the pile. The measured higher stress at the top of the pile than the bottom for low loads, and the subsequent strain softening are not predicted. This is probably because the direct shear test at low normal stresses needs too much movement to develop shear stress, and the soil deformation in this test does not adequately reproduce the sharply peaked slope of shear stress-movement graph that is clearly needed to reproduce the actual test values. There is scope here for further investigation into a more suitable shear test.

The proportion of total movement calculated to occur in the boundary layer region varied between 74% at the bottom of the pile at low loads, to 98% at the top of the pile at high loads. These proportions are high because of the very stiff nature of the undisturbed Gault clay. Figure 11 shows the predicted deformation profile in the highly stressed lower region of the pile, at $P_{ult}/2$. The shape of the profile, (apart from the proportion in the boundary layer), is similar to that measured round a pile loaded in another stiff clay by Cooke et al (1979). The proportion of boundary layer movement in their case was much less, probably because the surrounding soil had already been distorted (and hence softened) by jacking the pile into the ground. However the radial extent of significant distortion was very similar. Cooke et al measured it to be r_m = 9 pile

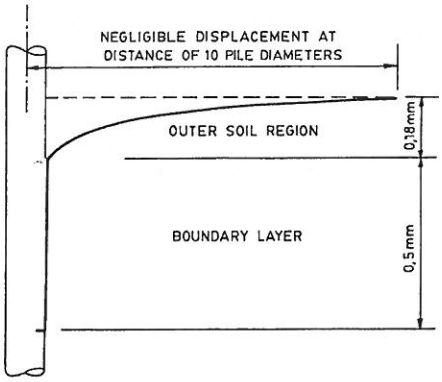

Fig. 11 - Calculated displacement profile.

diameters, whereas the present method predicted 10 diameters.

5. DISCUSSION AND CONCLUSIONS

The simple model of soil-pile behaviour described here has been shown to be capable of accurately predicting the performance of carefully installed piles, in a very uniform soil where a lot of soil test data was available. It requires the results of laboratory direct shear tests, and methods of determining in-situ values of K_o, shear stiffness and shear strength. The self-boring pressuremeter test has been shown to be capable of giving these parameter values.

The application of this model needs a computer, which is contrary to the philosophy expressed by Randolph and Wroth (1978), who deliberately made their theoretical developments to avoid the necessity for a computer. However, any desk-top computer is capable of doing the necessary calculations, and it is suggested by the present author that such machines are so widely available that the necessity for their use is justified by the more realistic nature of the three zone model (i.e. including the boundary layer) compared to Randolph and Wroth's two zone model.

Predicted design situations are such that the engineer will probably not have the uniformity of soil or quality of soil data that was the case for the test piles described in this paper, and consequently estimates based on previous experience will have to be made. It is further suggested that it is better for an engineer to accumulate such experience of parameter values for a soil-pile model that realistically represents actual behaviour.

6. REFERENCES

Cernica, J.N. 1982. Geotechnical Engineering. Tokyo:Holt-Saunders.

Cooke, R.W., Price, E. and Tarr, K. 1979. Jacked piles in London clay: a study of load transfer and settlement under working conditions. Geotechnique 29, No.2: 113-147.

Jardine, R.J., Maswoswe, J., Fourie, A. and Burland, J.B. 1985. Field and laboratory measurements of soil stiffness. Proc. 11th Int. Conf. on Soil Mech. and Found. Eng. V2:511-514.

Kay, J.N. and Parry, R.H.G. 1982. Screw Plate tests in a stiff clay. Ground Engineering. V15 No. 6:22-30.

Lee, I.K., White, W. and Ingles, O.G. 1983. Geotechnical Engineering. Boston: Pitman.

Murff, J.D. 1980. Pile capacity in a softening soil. Int. J. Num. and Anal. Methods in Geomechanics. V4:185-189.

Poulos, H.G. and Davis, E.H. 1968. The settlement behaviour of single axially loaded incompressible piles and piers. Geotechnique V18:351-371.

Randolph, M.F. and Wroth, C.P. 1978. Analysis of deformation of vertically loaded piles. J. Geotech. Eng. Div. A.S.C.E., V104, No.GT12:1465-1488.

Seed, H.B. and Reese, L.C. 1957. The action of soft clay along friction piles. Trans.A.S.C.E. 731-764.